

## A New Method for Analysis of Martials Nano and Micro Electronics Technologies

**Bassam Mohsin Atiyah**

Northern technical university & IRAQ- Kirkuk 36000

---

**ABSTRACT:** This final qualifying work investigates prospective microelectronic and nano electronic materials. The purpose of the final qualifying mission is to evaluate potential manufacturing technologies and materials. In the first phase of the endeavor, potential materials for microelectronics and nanoelectronics were investigated. Graphene, fullerenes, fullerites, carbon nanotubes (CNT), nanofibers, ferrites, barium hexaferrite, nano powders, and epitaxial coatings are among these substances. An investigation into diverse methodologies pertaining to the production of auspicious materials was undertaken during the preliminary stage of the undertaking. Molecular beam epitaxy, pulsed laser deposition, spray deposition, physical vapor deposition (PVD), chemical solution deposition, gas-phase synthesis, electrospinning, chemosynthesis, detonation synthesis and electric explosion, chemical vapor deposition (CVD), spray deposition, physical vapor deposition (PVD), and the sol-gel method were among these processes.

**KEYWORDS:** nanopowders, carbon nanotubes, chemical vapor deposition, nano electronic

---

### I. INTRODUCTION

Topic of research: Analysis of promising materials for micro- and nanoelectronics and technologies for their production The relevance of this topic is due to the fact that the unique properties of promising materials make them effective for widespread use in flexible electronics, nanoelectronics, energy conversion and storage devices, photonics and other promising areas The main goal of the study is to analyze promising materials and technologies for their production The objectives of the work are to consider promising materials for micro- and nanoelectronics, to study the technologies for their production and to analyze current research into the production of promising materials. Nanotechnology is a cognitive framework, despite the scientific community's fascination in nanoscience, the majority of current conversations, definitions, and concentration are directed towards nanotechnology. Therefore, it encompasses a wide-ranging concept that exemplifies the pinnacle of humanity's unending desire for knowledge with practical applications. Nanotechnology refers to the use of technology at the nanoscale to create functional structures by manipulating individual atoms and molecules, with practical applications in the real world [1]. Nanotechnology encompasses The conceptualization, construction, and application of chemical, physical, and biological systems with submicron-scale structural attributes, extending from atoms or molecules. Further, it involves the integration of the nanostructures that are produced into more extensive systems. [2], [3]. Nanotechnology may be defined as the use of technology at the nanoscale. Over time, several interpretations of nanotechnology have emerged. This first definition requires more elaboration, including the inclusion of a precise explanation of the concept of nanoscale. Therefore, it is essential to provide a clear definition of nanotechnology by first defining the term "nanoscale," which refers to a range of 1-100 nm. Nanotechnology may be defined as a technology that operates at the atomic level with exact control and manipulation of atoms. Nanotechnology is associated with systems and materials that have unique and greatly enhanced chemical, physical, and biological capabilities, processes, and phenomena due to their very small size at the nanoscale. Nanotechnology is defined as the process of designing, characterizing, manufacturing, and using materials at the nanoscale with precise control over their structure and size [5]. Another description provided by the same dictionary is "the deliberate and precise manipulation, accurate positioning, shaping, measurement, and fabrication of materials at the nanoscale in order to create substances, systems, and devices with fundamentally new properties and functions" [5]. Nanotechnology is an area of research that focuses on phenomena at the nanoscale, which is a very small size. It is a branch of knowledge that falls within the broader category of technology, specifically in the domains of colloidal science, chemistry, physics, biology, and other scientific disciplines.

**II. RESEARCH ANALYSIS**

Nickel ferrite nanofibers were synthesized by electrospinning. In [20], fibers with a diameter of 454-850 nm were synthesized. The fiber synthesis consisted of the following steps:

1. Preparation of a solution of nickel ferrite (NiFe<sub>2</sub>O<sub>4</sub>).
2. Synthesis of fibers using the electrospinning method.
3. Self-assembly of fibers in a magnetic field.

The electrospinning setup consisted of a syringe pump and a coaxial stainless steel needle with a diameter of 422 μm and a metal wall thickness of 140 μm. A high-voltage power The needle was supplied with the necessary voltage via a supply. A grounded collector in the shape of an aluminum cylinder was positioned 20 centimeters away from the needle's point. After transferring the nickel ferrite solution into 10 ml injectors via a syringe pump, the solution was injected at a rate of 0.3 ml/h into a coaxial needle. In order to gather fibers, the collector was rotated at the ideal velocity. The chamber's relative humidity was regulated to 30–40%. Twenty hours were spent drying the resulting fiber in an oven preheated to 50 °C, followed by one hour of firing at 650 °C in air.

Fig. 1(a) Shows uniform fibers 10–30 μm long. In pictures 1(b) and (c) show 2 types of fibers. Sample A – NFO shell (nickel ferrite) with a thickness of 125 nm and a PZT core (lead zirconate titanate) with a diameter of 200 nm; sample B – 1205 nm PZT shell and 450 nm NFO core.

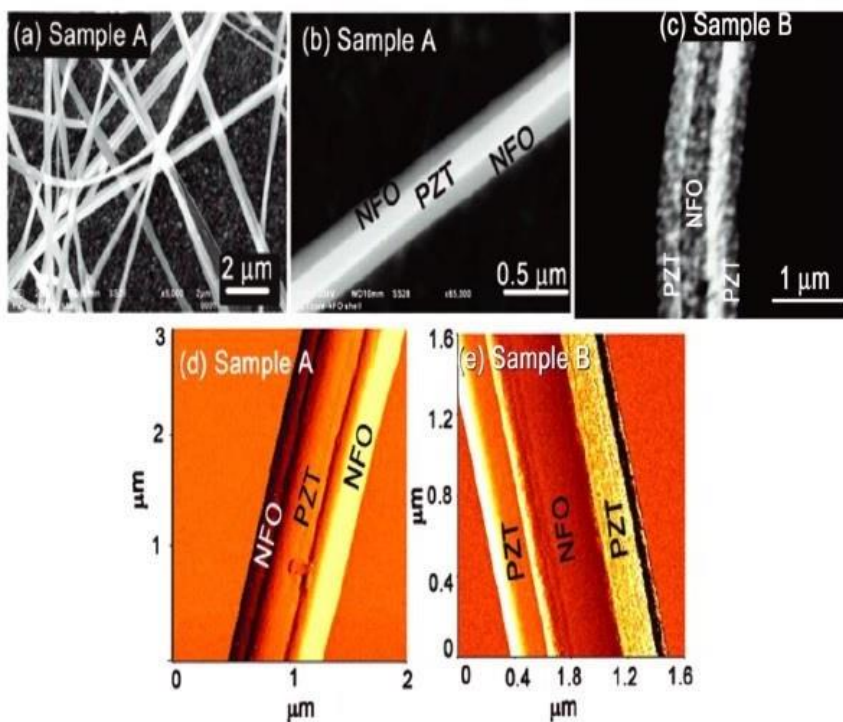


**Figure. 1 a – homogeneous fibers, b and c – samples A and B under a scanning electron microscope, d and e – samples A and B under a magnetic force microscope**

The magnetization measured using a Faraday balance for samples A and B is shown in Fig. 2(a). Both samples demonstrate a rapid increase in magnetization *M* with increasing magnetic field strength *H*. Fig. 2 (a) indicates magnetocrystalline anisotropy in the fibers.

In order to determine the ferroelectric properties of the fiber, its polarization *P* and electric field strength *E* were measured. Hysteresis is detected in both sample A and sample B in 2(c). Sample B, which contains 68% PZT by volume fraction, exhibits a greater polarization value *P* in comparison to sample A, which contains 20% PZT.

In both samples, the dependence of the polarization *P* on the magnetic field strength *H* was measured - Fig. 2.1.2(d). Both samples show an increase in polarization *P*. Since the change in polarization *P* induced by magnetic field strength *H* depends on the volume of ferrite, sample A with 80% NFO shows a greater change in polarization *P* than sample B with 32% NFO.

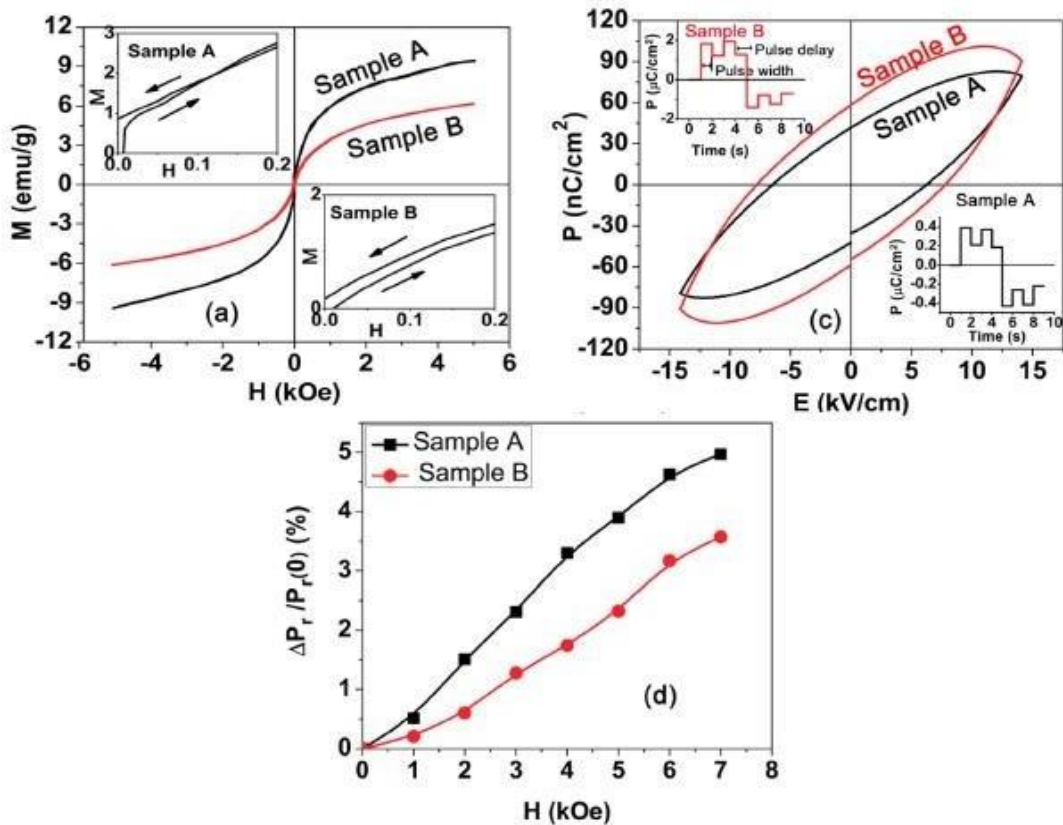


Figure. 2. a – dependence of magnetization  $M$  on magnetic field strength  $H$ , c – dependence of polarization  $P$  on electric field strength  $E$ , d – change in polarization  $P$  on magnetic field strength

Next, we consider fibers grouped under the influence of a magnetic field and their magnetoelectric characteristics under two types of conditions: in a uniform field and in a non-uniform field.

In Fig. Figure 3 shows samples obtained under a scanning electron microscope. In Fig. 3 (a) When subjected to a uniform field, the fibers of sample B become partially aligned in the field's direction. An analogous arrangement of fibers in the direction of the field is illustrated in Figure 3 (b) when sample B is present in low concentration. The formation of linear chains and the retention of fibers in specific regions are observed as the concentration of fibers in the solution increases, as depicted in Fig. 3 (c). These phenomena are attributed to the force exerted by the magnetic field gradient.

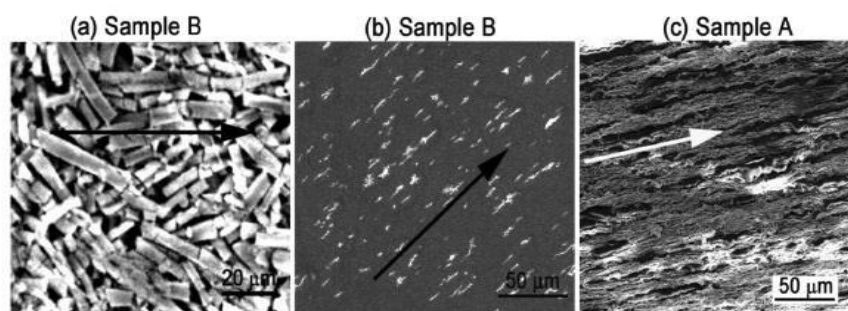


Figure. 3 Samples under a scanning electron microscope (arrows indicate the direction of the field): a – sample fibers subjected to a uniform magnetic field; B sample B fibers aligned parallel in a non-uniform magnetic field; c sample A fibers aligned in a non-uniform magnetic field.

### III. OBSERVED RESULTS

Nickel ferrite nanofibers were synthesized by electrospinning. The fibers were exposed to uniform and inhomogeneous magnetic fields, the dependence of polarization  $P$  on the electric field strength  $E$  and magneto-dielectric effects at a frequency of 20-22 GHz were studied. The magnetoelectric coupling of samples grouped under the influence of a magnetic field is stronger than that of ungrouped samples. Studies of polarization  $P$  induced by a magnetic field in grouped samples showed a decrease

## A New Method for Analysis of Martials Nano and Micro Electronics Technologies

and increase in polarization P depending on the nature of the fibers. Strong magnetoelectric interactions were detected with changes in permeability induced by a constant magnetic field H at 20–22 GHz.

Such fibers are of interest for use as magnetic sensors and microwave devices. [20]

Carbon nanomaterials are widely used as fuel cell electrodes, supercapacitor and battery electrodes, adsorbents, membranes, catalyst carriers, gas and liquid sensors. In most cases, the material requires high porosity, surface area and electrical conductivity. [8]

Samples of glassy carbon materials were obtained by thermolysis of furan polymers synthesized in a ternary system consisting of:

- furfuryl alcohol (FS),
- triethylene glycol (TEG),
- isooctylphenoldecaethylene glycol (IDEG)

with the addition of hydrochloric acid as a catalyst for the polycondensation of PS.

Heat treatment of polymer samples was carried out at 55, 89 and 150°C, holding for 20 hours at each temperature; the desiccated samples were then elevated to 9200°C at a rate of 50 K/h in the absence of oxygen for one hour. The compositions of the solutions utilized in the synthesis of furan polymers are illustrated in Figure 3. A circle delineates the area where materials with the most pronounced open bimodal porosity are formed.

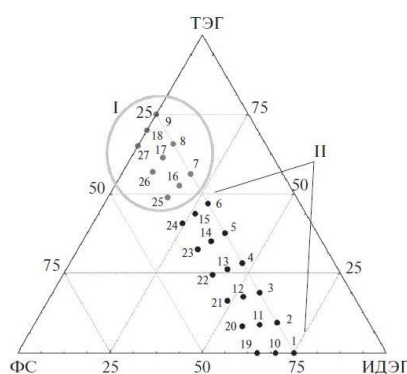


**Figure. 3** Scheme of the grid of solution compositions for sample synthesis; I – region of porous samples, II – region of dense cracked samples.

The samples had the shape of a parallelepiped and dimensions were 10 × 10 × 3 mm.

For further studies, 12 From this area, samples were selected (20–9, 16–18, 25–220, and 34–36). Samples 34–36, which were not depicted in the diagram, were distinguished from samples 16–18 by the incorporation of carbon nanotubes at a concentration of 1% by weight of amorphous carbon. The materials derived from solutions outside the delineated region are uninteresting due to their density being nearly equivalent to that of non-porous amorphous carbon. [8]

### III.2. Conducting an experiment

Electron microscopic studies made it possible to establish It was observed that samples acquired open porosity in all series from solutions containing the highest concentration of TEG. This property resembles a spatial network of vitreous carbon grains connected by bridges, as illustrated in Figure 4.

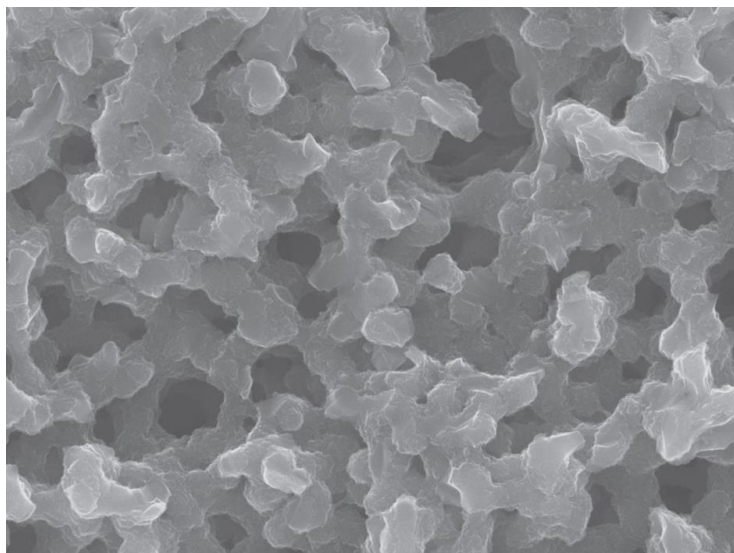


Figure. 4 according to electron microscopy the Morphology of sample C26.

The images of the wafers provide an approximation of 0.1–6 μm for the mean size of the granules that comprised the spatial network. The porous structure of these materials facilitates the unimpeded passage of liquids and gases into the sample's deep layers. This characteristic renders them highly auspicious for applications such as adsorbents, membranes, catalyst carriers, supercapacitor electrodes (electrochemical capacitors, double-layer capacitors), gas sensor components, and fuel cell electrodes.

A significant benefit of the acquired materials is their elevated electrical conductivity, which is a result of bridges connecting all grains within a monolithic carbon framework. This is in contrast to the majority of established electrode materials derived from powders, which rely solely on point contact between grains. 2–6 ohms is the resistance between the opposite faces of parallelepipeds measuring 10 10 3 mm.

By comparing the dimensions of large pores as determined by electron microscopy data with the dimensions of mesopores as determined by nitrogen adsorption data, it is possible to deduce that IDEG has the opposite impact on the development of large and small pores in the glassy carbon materials that result (see Figure 5). IDEG facilitates the enlargement of micropores and mesopores while simultaneously diminishing the dimensions of crystalline carbon granules (droplets within an emulsion of PS oligomers in solution). The initial factor that explains both phenomena is the greater solubility of oligomers in IDEG as opposed to TEG.

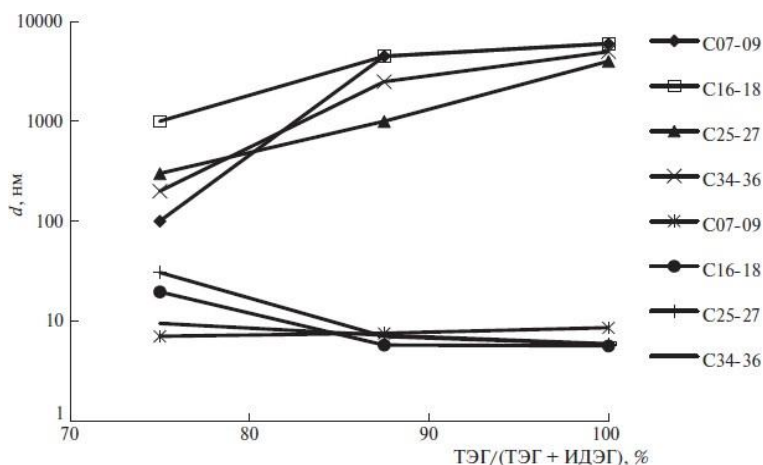


Figure. 5 Dependence of pore size (d) on the composition of the initial solutions (TEG/(TEG + IDEG)).

Microporosity, apparently, is an additional outcome resulting from IDEG's favorable solubility in the furan polymer. Micropores are produced when molecules of low molecular weight substances dissolved in a cross-linked polymer are removed by heating. The oligomer appears to dissolve entirely in this mixture at a TEG/(TEG+IDEG) ratio of 0–65%. Heating the solution induces the solvents to evaporate, followed by the formation of a densely fractured polymer and crystalline carbon. By

## A New Method for Analysis of Martials Nano and Micro Electronics Technologies

manipulating the quantity of a particular solvent within the solution, it is possible to gradually alter the structure of the resultant carbon that resembles glass.

To facilitate the operation of a substance as an electrode for a fuel cell, it is optimal to possess sizable apertures that permit easy liquid access.

### III.2.3. Observed results

The resulting glassy carbon materials revealed the presence of macropores with sizes of 0.1–6  $\mu\text{m}$ , meso- and micropores with sizes of 1–50 nm. In this case, the surface area, pore diameter and total porosity depend on the ratio of TEG and IDEG in the initial solutions.

When the TEG/(TEG+IDEG) ratio is in the range from 205 to 100%, with a decrease in TEG content, the sizes of macropores decrease and the sizes of micropores increase.

When the ratio TEG/(TEG + IDEG) is from 0 to 62.5%, bimodal porosity disappears, and non-porous, dense materials are formed.

Analysis of voltammograms showed that an increase in the surface area of the material leads to an increase in the density of currents flowing through the electrode. For electrochemical applications, samples with a predominance of micropores and a high surface area have the optimal set of characteristics, which in the future makes it possible to use them as carriers for catalysts in fuel cells, sensors and batteries. [8]

### III.3. Microporous glassy carbon materials

The advantages of microporous glassy carbon samples are high specific surface area, chemical inertness and electrical conductivity. These properties are well suited for the production of electrodes for ultra-high capacitance capacitors, electrochemical and fuel cells, adsorbents, molecular sieves, membranes, catalysts and carriers for catalyst particles [9].

#### III.3.1. Sample technology

Samples of glassy carbon materials were obtained by thermolysis of furan polymers synthesized in a ternary system consisting of:

- furfuryl alcohol (FS),
- triethylene glycol (TEG),
- liquid nonionic surfactant – polyethylene-10-glycol ether of isoocetylphenol (trade name OP-10).

**Table 1 – Composition of the initial solution for synthesis and properties of the resulting glassy carbon samples**

Sample	Composition of the initial solution		
	FS	OP-10	Zero
AS1	70.0	30.0	0
AS5	70.2	0	29.8
AS6	50.0	50.0	0
AS10	50.5	0	49.5
AS11	30.0	70.0	0
AS12	30.1	52.4	17.6
AS13	30.0	35.0	35.0
AS15	30.9	0	69.1
AS16	100	0	0

An appropriate solution based on TEG and OP-10 (with 0, 20, 40, 205 and 100 wt.% TEG) in the required amount was added to portions of 5 g of PS, mixed, after which a few drops of 20 wt.% were added. % sulfuric acid to catalyze the polycondensation reaction of the PS.

Following an 18-day polymerization period at room temperature, the specimens were desiccated in an oven preheated to 55°C, 89°C, and 150°C for 20 hours each.

## A New Method for Analysis of Martials Nano and Micro Electronics Technologies

Following dehydration at 150°C, the specimens were subjected to oxygen-devoid heat at a rate of 50 K/h, increasing to 9200°C, where they were calcined for one hour.

The substances calcined were black carbon samples [9]

### III.3.2. Conducting an experiment

Depending on the composition of the initial solutions, the resulting samples of glassy carbon materials acquire different morphologies (Fig. 6).

By acquiring the morphological characteristics of the initial two liquid phases that were generated in the intermediate phase of furan polymer formation, glassy carbon presents a distinctive opportunity to employ an electron microscope for the examination of the interface between two liquids. The calcined material does not contain the second liquid, which is composed of water and inserted low molecular weight liquids that were liberated during the polycondensation process of furfuryl alcoho I, whereas the first liquid is composed of furan resins (oligomers). Prior to the addition of acid and during the early phases of polymerization, a homogeneous solution is formed by combining all three liquids (FS, OP-10, and TEG) in any proportion. Phase separation occurs at a specific juncture due to the decrease in solubility of PS poly's oligomers in low molecular weight solutions (PS, OP-10, TEG, and water) as PS poly condenses. Although each phase comprises these components in different proportions, the polymer predominates over low-molecular-weight substances. The morphological transformation of the resulting polymer into a dispersed phase (droplets) or a dispersion medium (containing droplets of low-molecular substances) is contingent upon the concentration of PS in the initial solution.

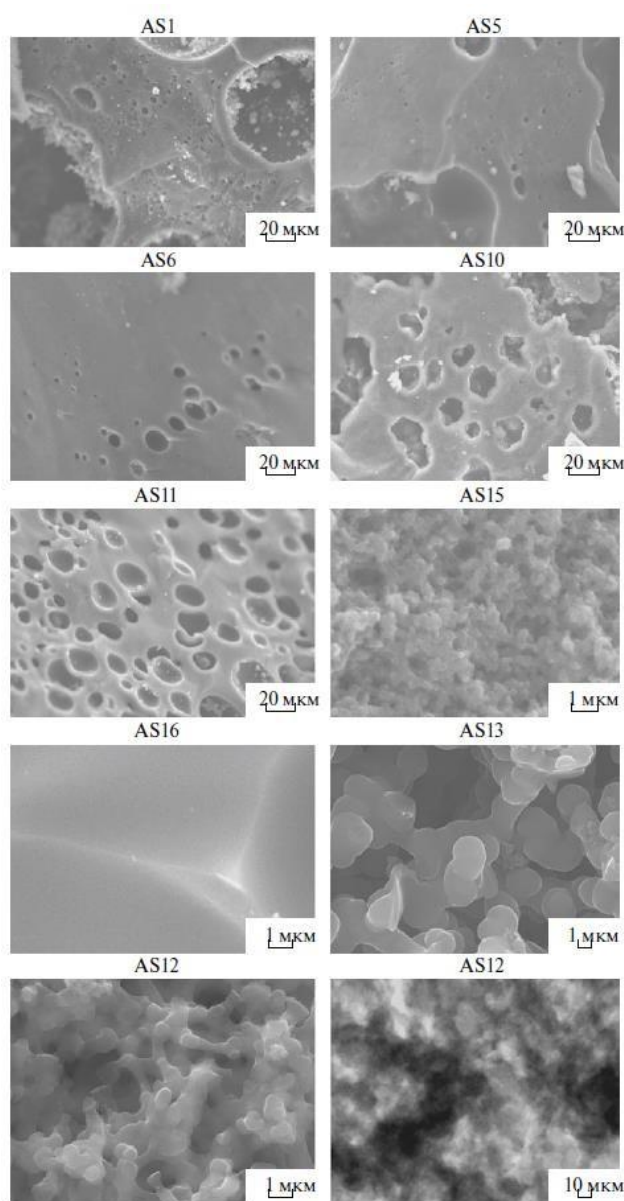


Figure. 6 Structure of samples according to scanning and transmission (AS12) electron microscopy data.

## A New Method for Analysis of Martials Nano and Micro Electronics Technologies

When the interfacial tension between liquids is diminished, such as when surfactants are introduced, the interface becomes more pronounced, resulting in reduced droplet size and a coarser surface texture of the droplets. Under these circumstances, both phases are capable of combining to form a bicontinuous structure, wherein the complete volume of the sample can traverse any of the phases without encountering interphase boundaries.

This morphological variant is observed in samples AS12, AS13, and to a lesser extent, AS15. They are composed of a connected three-dimensional network of polymer particles that undergo a transformation into glassy carbon through the process of discharge (see Figure 2.3). The aforementioned porous configuration enables the ingress of gas or liquid molecules into the resultant substance. As for samples AS12, AS13, and AS15, the mean droplet size is 0.8  $\mu\text{m}$ , 1.5  $\mu\text{m}$ , and 0.3  $\mu\text{m}$ , respectively.

Finer details of the internal structure of AS12 particles become visible at a magnification of 500000 (see Figure 2.3). Every *particle of the calcined polymer exhibits characteristics of foam that are created by deformed single-layer and multilayer graphene sheets*. As with activated carbons, the term "crumpled paper model" can be used to describe the morphology of the internal structure of particles. The mesopores that have been observed in AS12 range in size from 2 to 20 nanometers. Additionally, the substantial benzene adsorption indicates the existence of micropores smaller than 2 nm.

It is possible to estimate the geometric surface area of samples, which are microspheres as an initial approximation, by utilizing information regarding their diameter and density. Therefore, the density of the crystalline carbon in sample AS16 is 1.53 g/cm<sup>3</sup>, while the diameter of the microspheres in sample AS12 is 0.8  $\mu\text{m}$ . One microsphere has a mass of  $6.18 \times 10^{-13}$  m<sup>2</sup> and an area of  $15.4 \times 10^{-12}$  m<sup>2</sup>. Thus, presuming that these microspheres are devoid of cavities, their specific surface area is 25 m<sup>2</sup>/g. By comparing the estimation derived from geometric dimensions to calculations utilizing the adsorption value of benzene (805 m<sup>2</sup>/g for AS12), it is possible to deduce that the microsphere material lacks density but harbors a considerable quantity of mesopores and micropores (approximately 2080 m<sup>2</sup>/g in area for AS12 [9]).

### II.3. Observed results

As determined by mechanical property measurements, a plate cut from sample AS13 with a thickness of 3 mm exhibited remarkable qualities: a compressive strength of 60 MPa, an elastic deformation of 1.8%, and an elastic modulus of 3.1 GPa. This suggests the potential applications of this substance in the fabrication of devices that utilize adsorption, catalysis, electronic, and electrochemical processes. The proposed synthesis method makes it possible to obtain these materials in the form of large products (blocks, disks, cylinders, pipes). [9]

### II.4 Preparation of nanofibers by electrospinning

Modern carbon nanofibers (CNFs) do not yet have high tensile strength. But the electrospinning process makes it possible to obtain CNFs with a diameter of 150–500 nm with unique properties due to their continuous and combined shapes, which is useful when using CNFs in composite materials.

#### II.4.1. Sample technology

The article [10] discusses the process of producing high-strength nanofibers with a carbon content of up to 90% using the electrospinning method.

Electrospinning is the process of forming nanofibers as a result of electrostatic forces on an electrically charged stream of a polymer solution or melt.

The material used to make the nanofibers consisted of polyacrylonitrile containing 94.6% monoacrylonitrile and 5.4% onomethyl acrylic.

The solution supplied by a pump through a capillary using a dispenser is exposed to a voltage of 10...60 kV. The voltage is regulated by a high voltage source. It induces electric charges of the same sign in the polymer solution, due to which the polymer solution is stretched into a thin stream. During the electrostatic drawing process, the polymer jet can be divided into thinner jets. The material then enters the manifold regulator. The solution from the pump is sprayed onto the collector.

The resulting jets harden during the evaporation of the solvent or as a result of cooling, turn into fibers, and, under the influence of electrostatic forces, drift to a grounded substrate, which has the opposite sign of the electric potential.

The nanofibers are stabilized in an oven by heating at a rate of 5 °C/min to 300 °C and then held at that temperature for 1 hour.

#### II.4.2. Conducting an experiment

Stabilized nanofibers were deposited on foil and placed in a high-temperature carbonization oven. The nanofibers are heated for 1 hour (at maximum temperatures of 800 °C, 1100 °C, 1400 °C, and 12000 °C) to determine how carbonization temperature affects tensile strength and elastic modulus. Heating rate 5°C/min.

## A New Method for Analysis of Martials Nano and Micro Electronics Technologies

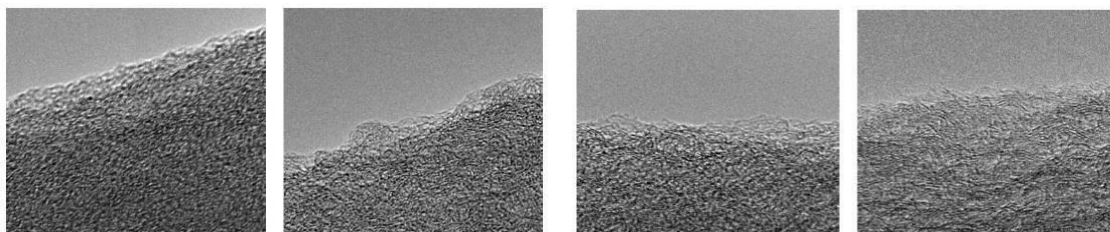


Figure. 7 Nanofibers obtained by electrospinning (a), fibers stabilized at  $290 \pm 20 \text{ }^\circ\text{C}$  (b), carbonization of nanofibers at  $800 \text{ }^\circ\text{C}$  (c), carbonization at  $12000 \text{ }^\circ\text{C}$  (d)

Different conditions of the electrospinning process affect the diameter of nanofibers. Relative humidity also affects the morphology of nanofibers. Nanofibers formed at 60% relative humidity had a rough surface and porosity, while those formed at 30% relative humidity had a smooth surface.

Table 2 – Diameter of nanofibers under various electrospinning conditions

Voltage, kV	Distance to collector, cm	Diameter of nanofibers, nm
25	25	430
20	20	450
16	15	4200
25	20	390
20	25	530
25	15	430

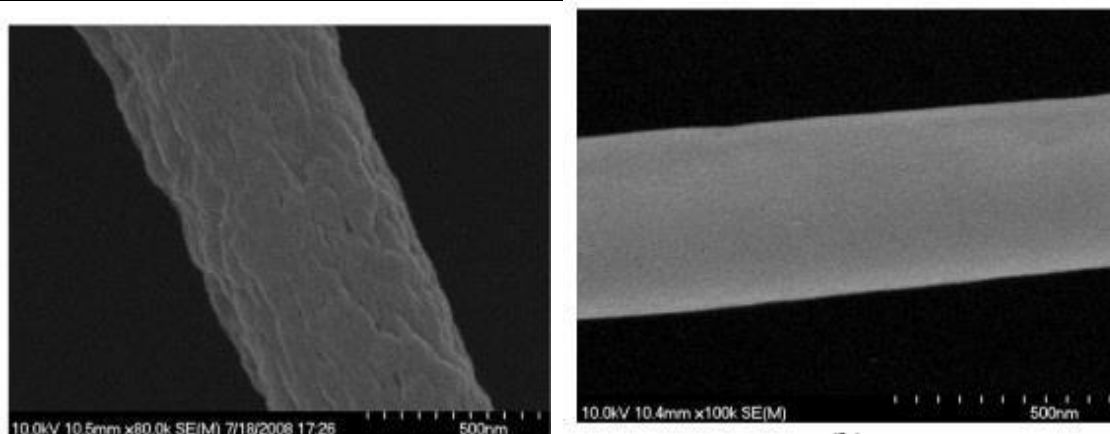


Figure. 8 Surface of nanofibers at humidity 60% (a) and 30% (b)

CNFs produced by the electrospinning process are unique compared to existing carbon nanofibers and nanotubes because they have continuous and combined shapes, which is advantageous when used in composite materials.

The ultimate strength of carbon nanofibers reaches a maximum of 3.6 hPa at  $1400 \text{ }^\circ\text{C}$ , the elastic modulus increases to  $12000 \text{ }^\circ\text{C}$  and is equal to  $1202 \pm 40 \text{ hPa}$ , which is 600% and almost 300%, respectively, with respect to previously reported data.

Also, such carbon nanofibers have uniform cross-sections and, as a result, improved mechanical properties, which can improve the efficiency of aircraft structures. [10]

### IV. CONCLUSIONS

Nickel ferrite nanofibers were obtained by electrospinning. Such nanofibers have high magnetoelectric properties, which makes it an effective material for designing microwave devices.

Porous glassy carbon nanomaterials were obtained by thermolysis. Heat treatment of the polymer mixture made it possible to obtain glassy carbon samples with micropores.

Glassy carbon nanomaterials obtained by this method have chemical inertness and high electrical conductivity. These properties are useful in the production of electrodes for ultra-high capacitance capacitors, electrochemical and fuel cells, adsorbents, molecular sieves, membranes, catalysts and carriers for catalyst particles.

## A New Method for Analysis of Martials Nano and Micro Electronics Technologies

Carbon nanofibers were obtained by electrospinning. The polymer solution was subjected to tension, causing it to stretch into thin streams that fell on the collector. Then the jets are cooled and nanofibers are obtained.

Carbon nanofibers obtained through the electrospinning process have continuous and combined forms; their strength, elastic modulus and other properties allow them to be effectively used in many areas, for example, in the production of composite materials.

### REFERENCES

- 1) McNeil, S. E. (2005). Nanotechnology for the biologist. *Journal of leukocyte biology*, 208(3), 585-594.
- 2) Emerich, D. F., & Thanos, C. G. (2003). Nanotechnology and medicine. *Expert opinion on biological therapy*, 3(4), 655-663.
- 3) Ramsden, J. (2016). *Nanotechnology: an introduction*. William Andrew.
- 4) Nasrollahzadeh, M., Sajadi, S. M., Sajjadi, M., & Issaabadi, Z. (2019). An introduction to nanotechnology. In *Interface science and technology* (Vol. 28, pp. 1-220). Elsevier.
- 5) Roco, M. C. (2011). The long view of nanotechnology development: the National Nanotechnology Initiative at 10 years. *Journal of nanoparticle research*, 13, 4220-445.
- 6) Heath, J. R., & Davis, M. E. (2008). Nanotechnology and cancer. *Annu. Rev. Med.*, 59, 251-265.
- 7) Bhushan, B. (Ed.). (2012). *Springer handbook of nanotechnology*. Springer.
- 8) Silva, G. A. (2004). Introduction to nanotechnology and its applications to medicine. *Surgical neurology*, 61(3), 216-220.
- 9) Mahalik, N. P. (2006). *Micromanufacturing and nanotechnology* (pp. 1208-180). Berlin: Springer.
- 10) Service, R. F. (2004). Nanotechnology grows up.
- 11) Brumfiel, G. (2003). Nanotechnology: A little knowledge... *Nature*, 420(6946), 206-209.
- 12) Brune, H., Ernst, H., Grunwald, A., Grünwald, W., Hofmann, H., Krug, H., ... & Wyrwa, D. (2006). *Nanotechnology: assessment and perspectives* (Vol. 220). Springer Science & Business Media.